Available online at www.eccomasproceedia.org
Eccomas Proceedia COMPDYN (2017) 4869-4880

ECCOMAS
Proceedia

COMPDYN 2017
6th ECCOMAS Thematic Conference on
Computational Methods in Structural Dynamics and Earthquake Engineering
M. Papadrakakis, M. Fragiadakis (eds.)
Rhodes Island, Greece, 15–17 June 2017

NUMERICAL MODELLING AND CALIBRATION OF RC COLUMNS UNDER AXIAL LOADING

Tuba Tatar[1], **Mário Pimentel**[2], **José Miguel Castro**[3] and **Mário Marques**[4]

[1] University of Porto
Porto, Portugal
e-mail: tuba.tatar@fe.up.pt

[2] University of Porto
Porto, Portugal
e-mail: mjsp@fe.up.pt

[3] University of Porto
Porto, Portugal
e-mail: jmcastro@fe.up.pt

[4] University of Porto
Porto, Portugal
e-mail: mario.marques@fe.up.pt

Keywords: Numerical modeling, column, axial load, calibration

Abstract. *This work presents the first step of a methodology to calculate monetary losses in reinforced concrete moment resisting buildings through an innovative and advanced methodology. This framework involves the correlation between the physical damages that a structural component may experience during seismic events with meaningful engineering demand parameters. The establishment of this correlation constitutes the first phase of the methodology and is obtained through detailed finite element simulations of the critical structural elements. In this paper the development of numerical modeling strategies for the detailed simulations of five columns are described. The paper describes step by step the whole calibration process involving mesh sensitivity studies, evaluation of the influence of the compression fracture energy, geometric nonlinearity, bond-slip action and the buckling of the compressed reinforcements. In order to simplify the problem, pushover analysis is adopted to analyze all the models.*

Peer-review under responsibility of the organizing committee of COMPDYN 2017.
doi: 10.7712/120117.5768.18230

1 INTRODUCTION

Seismic risk assessment provides the first step for understanding the impact of earthquakes and determining the need of seismic rehabilitations. It is significant as well as for pre-earthquake preparedness and awareness in terms of human and economic losses. The assessment process provides meaningful information to stakeholders and decision makers on the seismic risk level of the structure portfolios and leads them to step towards rehabilitation and retrofitting process if necessary.

In current pre-earthquake loss assessment approaches, damage is commonly defined based on ductility ratio (maximum displacement over yielding displacement) or dissipated energy and usually related with either global or local indices [1-4]. The indices can provide an indication of the vulnerability of the structure, performance evaluation of the structure and decision regarding to rehabilitation of the structure. Even though the indices are able to indentify non damaged and severely damaged elements, they, however, poorly provide accurately results for intermediate damage states, which is the most critical stage regarding of the need for strengthening [5]. To improve the accuracy of economic loss predictions in RC frame buildings, an advanced methodology is proposed.

This methodology consists of two main phases, the first of which requires the identification of physical damages using detailed finite element analysis of critical structural elements. These damages are then correlated with meaningful engineering demand parameter(s) which shall be also suitable on the simplified models that can be used for assessing reinforced concrete buildings under seismic action. The monetary losses are determined based on the damages defined in the first phase. This new methodology allows users calculating monetary loss directly without using consequence function. The damage scales are redefined by experts in terms of the physical damages and cost of repair is redefined according to the available applied repair techniques in the new procedure [6]. Additionally, the damage limit states are calculated for each structural component individually and it improves the accuracy of monetary loss calculation. This methodology can be applied on flexural controlled reinforced concrete moment resisting frame structures regardless of height or irregularity.

Reproducing the experimental results not only in terms of global response, but also in terms of the physical damages is crucial and affects the accuracy of the methodology. Thus, a systematic calibration process is developed and exemplified here for the numerical models of columns and five parameters are investigated: mesh sensitivity, compression fracture energy, geometric nonlinearity, bond-slip and Dhakal-Maekawa post-yielding buckling.

2 NUMERICAL MODELING OF THE COLUMNS

The methodology is applied to five different columns, which are modeled and assessed numerically using software DIANA 9.6 [7]. These specimens were previously tested in laboratory: one is at University of Porto (UP) [8], the remaining ones (V1, V2, V3 and V4) are selected from the literature [9]. The geometrical and material properties of the columns are provided in Table 1.

Concrete is modeled using 20 node brick elements with (CHX60) with 3x3x3 Gauss points. The total-strain rotating smeared crack model available in DIANA material library is selected as constitutive model for concrete. The analyses start using Von Mises plasticity for reinforcing bars. The Dhakal-Maekawa constitutive model is employed for the bars under compression in order to model the effects of rebar buckling. Figure 1 shows the numerical models of the specimens, the red lines in (a) and (c) represent the reinforcing bars and (b) and (d) illustrate the meshed models. The analyses are carried on under monotonic loading whereby as-

suming that envelop of cyclic loading is represented by the monotonic force-displacement curve.

Specimen No.	***Section*** *mm²*	***Height of the column*** *mm*	***f_c'*** *N/mm²*	***f_y*** *N/mm²*	***Axial Load*** *kN*	***Long. Rein.***	***Stirrups*** *Ø/mm*	***Rein. Ratio (ρ) %***	***Mech. Rein.Ratio (ω) %***
UP	200x400	1500	48	436	170	6Ø12	Ø6/150	0.85	8
V1	300x300	1100	30	344	0	12Ø13	Ø6/70	1.77	20
V2					310				
V3					620				
V4					930				

Table 1: Geometrical and material properties of the specimens

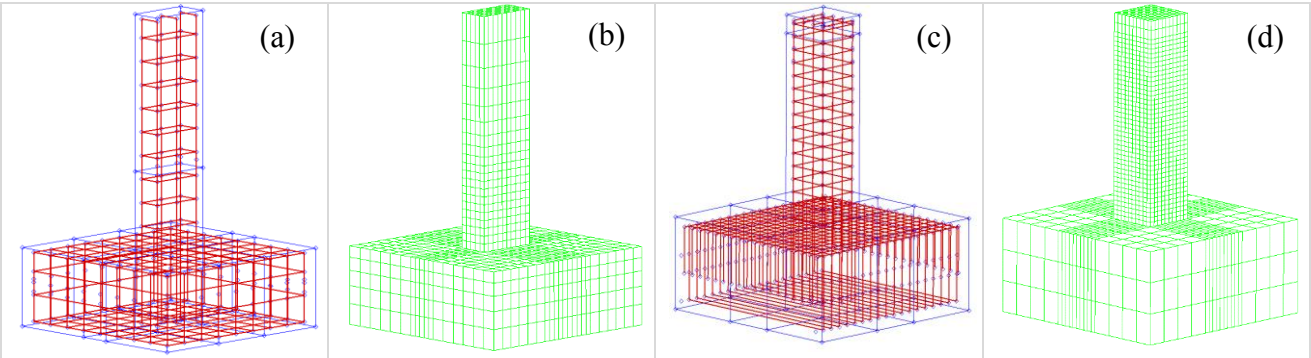

Figure 1: Reinforcement bar (a) and meshed model (b) of UP, reinforcement bar (c) and meshed model (d) of V1,V2V3 and V4

3 CALIBRATION PROCESS

As the first phase of the methodology relays on reproduction of the experimental results, a systematic calibration process was employed. This process includes 5 main steps in order to assess the influence of the mesh refinement, compression fracture energy, geometric nonlinearity, bond-slip between the rebar and the concrete and Dhakal-Maekawa post-yield buckling in the compressed rebar. Each of these steps is discussed in detail below.

3.1 Mesh Sensitivity

In finite element analyses, the size of the elements may influence the response and selection of the mesh sizes may govern the accuracy of the results. In quasi-brittle materials like concrete, which exhibit strain softening behavior, regularization procedures based on the definition of tensile and compressive fracture energies are adopted in order to reduce and nearly eliminate mesh size dependency of the results. In order to select adequately sized meshes and to assess the influence of the chosen mesh size on the global response, three different mesh sizes are investigated for each type of the column:

1. UP:

40x35x40 mm^3, 67x70x80 mm^3 and 67x140x200 mm^3 respectively for fine, medium and coarse volumes

2. V1, V2, V3 and V4:

25x30x25 mm^3, 50x60x25 mm^3 and 100x100x100 mm^3 respectively for fine, medium and coarse volumes.

Figure 2 shows the results of mesh size sensitiveness study for the five columns in terms of shear vs. displacement. Influences of the axial load level on the response objectivity can be observed on V3 and V4, the columns with higher axial load levels. In these analyses the ductility is clearly governed by concrete crushing, which occurs earlier in the models with coarser meshes. This is due to the fact that the finer the mesh is, the sooner the peak compressive stress is achieved in virtue of the of the higher accuracy in reproducing the pre-peak stress and strain fields in the most stressed regions of the column. Therefore, even if regularized (mesh-objective) stress-strain curves are employed for concrete in compression using the concept of compressive fracture energy, still a moderate degree of mesh dependency should be expected in the structural response. On the specimens with lower axial load levels (UP, V1 and V2), the mesh size dependency on the ductility is not as noticeable

Due to stability concerns in further analyses and crack pattern evaluations with experiments, the fine sized mesh is selected for all the models even tough medium seized mesh would provide objective results.

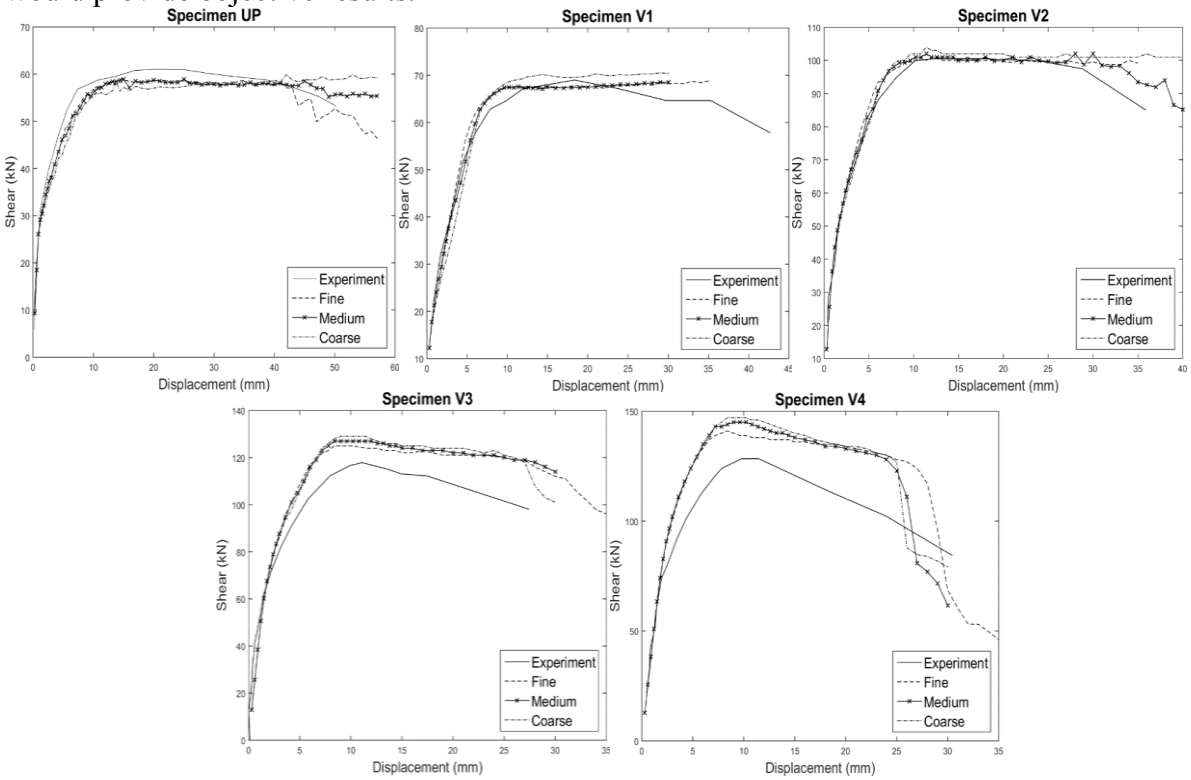

Figure 2: Mesh sensitivity investigation

3.2 Compression Fracture Energy (G_c)

When modelling concrete fracture with continuum elements, it is well known from nonlinear fracture mechanics that after reaching the maximum stress, the stress-strain relation cannot be considered a material property anymore. Two additional parameters are required, the fracture energy and a characteristic length, which in the case of the adopted modelling strategy, is related to the finite element size. In the case of tensile fracture, the fracture energy G_f is defined as required energy to open a crack within a unit length. In the case of compressive fracture, the compressive fracture energy G_c can be defined as the required energy to crush (until full stress release) a unit area perpendicular to the principal compressive stress. The first estimated G_c value is gradually increased until the ductility of the specimen is captured. Effects of compression fracture energy are shown in Figure 3with reference to shear and displacement. Compression fracture energy influence can be observed intensely only if there is concrete

failure. The specimen V1 with variant G_c is able to reproduce the same results and even the smallest given G_c is sufficient under the applied load. Concerning higher axial load level, the failures of models with small G_c are, however, observed earlier as seen especially in V3 and V4. If ductility is concerned and required to be matched to experimental results, playing with compression fracture energy would be an option for users.

Thus, the selected G_c value for V1, V2, V3 and V4 is 80 N/mm and for UP is 50 N/mm whereas those values are able to reproduce the ductility of the specimens and following investigations have been proceeded using those values.

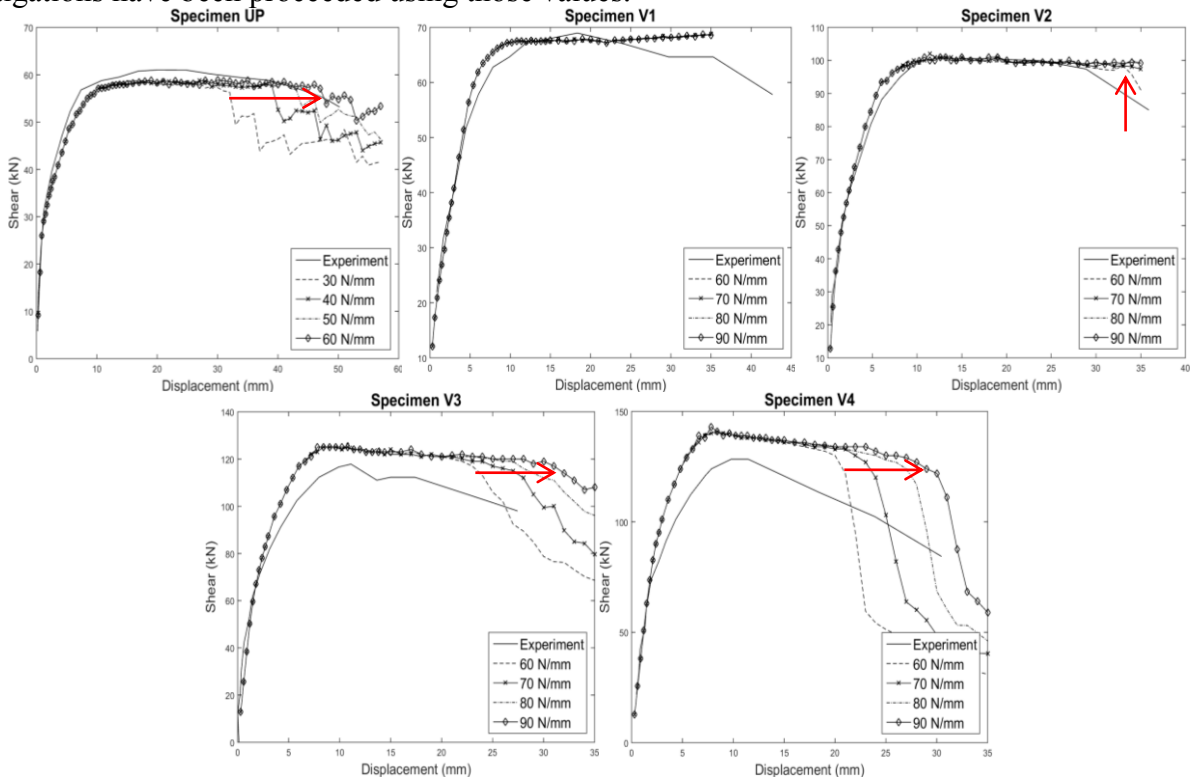

Figure 3: Compression fracture energy effects on global response

3.3 Geometric Nonlinearity

Geometric nonlinearity is an important parameter in this study. If there is axial load, especially high level, the P-Δ effect must be taken into account since the second order bending moments are not negligible. Secondly, considering geometric nonlinearity is very essential if the buckling of rebar is considered explicitly in the analysis.

Figure 4 illustrates the geometric nonlinearity influences on global response of the specimens. After including the parameter into the analyses, the maximum value and also ductility are influenced immensely. The impact of the parameter growths visibly while the axial load level increases as seen on V3 and V4. Over all, and as should be expected, geometrical nonlinearity analyses produce more consonant results to the experiments.

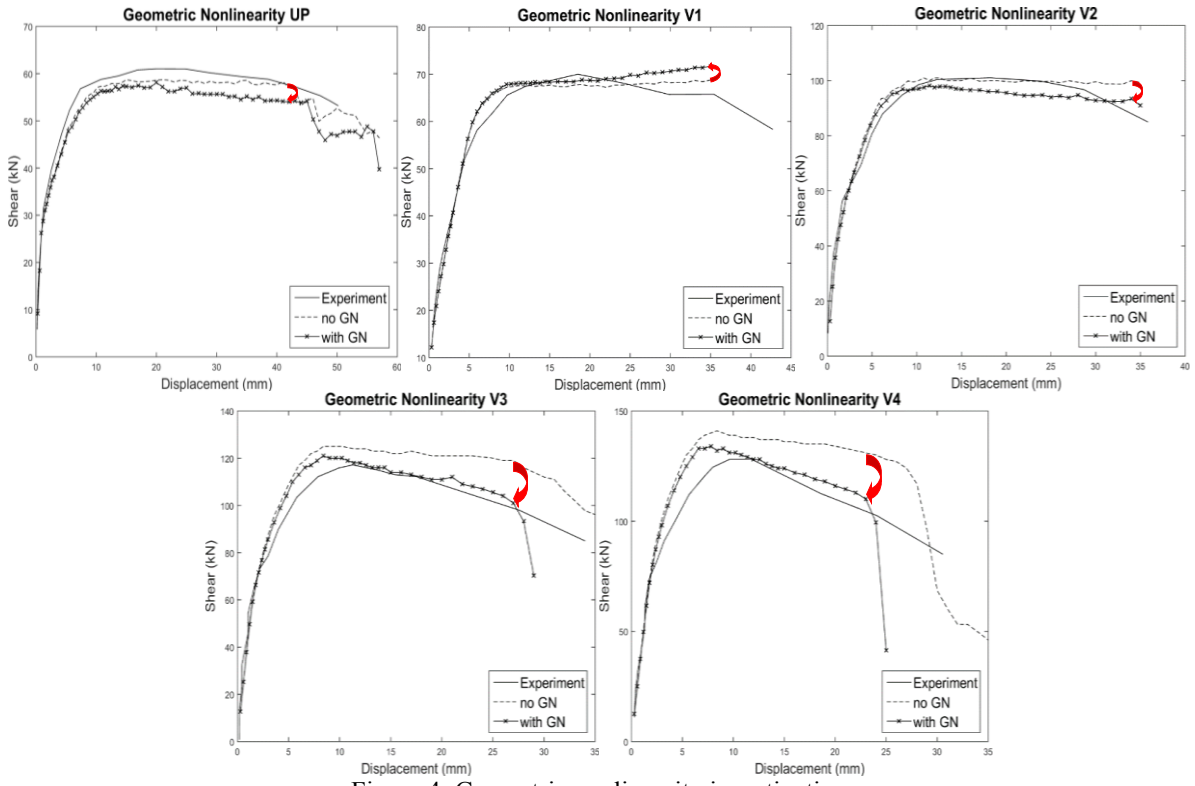

Figure 4: Geometric nonlinearity investigation

3.4 Bond-Slip Influence

After cracking, relative displacements (slip) and bond shear stresses develop along the interface between concrete and steel. With increasing load and eventual yielding of the rebars, the reinforcing bar slip increases even more. This phenomenon can be modeled explicitly using interface elements and bond shear stress-slip constitutive laws and is important for the consistent determination of the crack spacing and of development of the plastic hinge. In the present study, the constitutive model for bond-slip proposed in the CEB-FIB 1990 is adopted, which depends on the concrete strength, confinement effect and rib length [10]. According to the constitutive relation given onto the interface element, the steel and the concrete elements are not forced to act compatible anymore and a slip between two materials is allowed. In the numerical models, tangential traction values (bond-slip values) of the interface elements are calculated using CEB-FIB equation. The behavior of interface elements is given in Figure 5 . There are four possible scenarios: “confined-good”, “confined-other”, “unconfined-good” and “unconfined-other” bond condition. Each of these bond and confinement conditions is applied on the models separately.

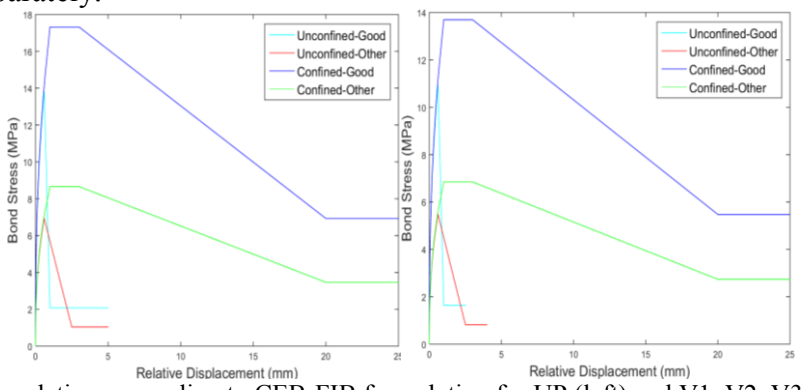

Figure 5: Bond-slip relations according to CEB-FIB formulation for UP (left) and V1, V2, V3 and V4 (right)

Figure 6 shows effect of those four conditions for each column also including the result without bond-slip activation and the experimental response in terms of shear vs. displacement. The arrow on the graphs indicates roughly the yielding point of the rebar. The responses are clearly affected around the yielding points after including the bond-slip interface constitutive model. A reduction in response can be also observed whereby the rebar is not forced to be compatible with concrete. Moreover, improvement in ductility can be observed especially on the example with higher axial load level. Importantly, the plastic hinge length decreases due to damage localization on the models which also helps to form more realistic crack pattern along the tension side of the columns. The most fitted condition is selected for the specimens, which is the "confined-other" bond condition for the models and following analyses are carried out using the selected condition.

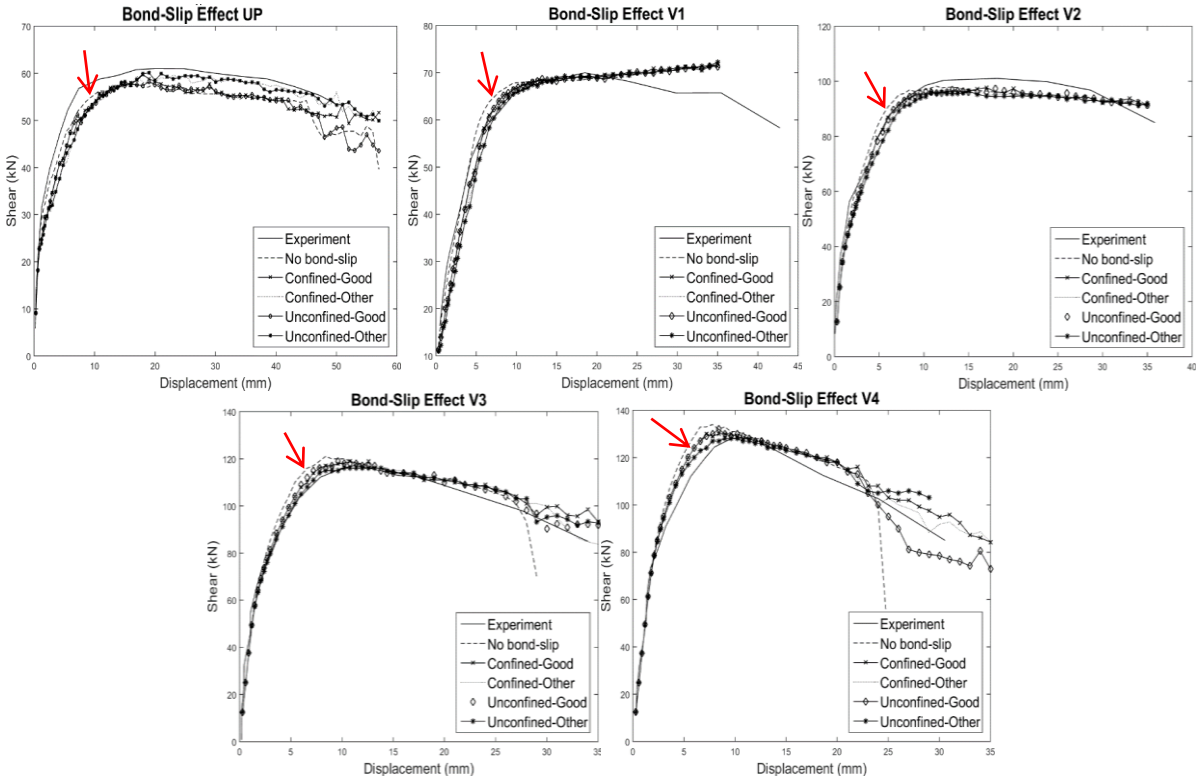

Figure 6: Influence of Bond-Slip Action of Global Response

3.5 Dhakal-Maekawa Post-Yield Buckling

Dhakal and Maekawa investigated post-yield buckling in bare steel bars and proposed a constitutive model shown in Figure 7 (a) [11] which includes the influence of rebar length, diameter and yielding strength. This model introduces post-yield buckling behavior to the compressed steel bars via a modification of the uniaxial stress-strain curves. Figure 7 (b) displays the calculated values according to the proposed model for reinforcing bar. Since the stirrup spacing of UP is 15 cm, the influence of buckling can be dramatically observed after yielding point. The stirrup spacing for the remaining specimens is, however, equal to 7 cm and the reduction in stress due to buckling remains mild.

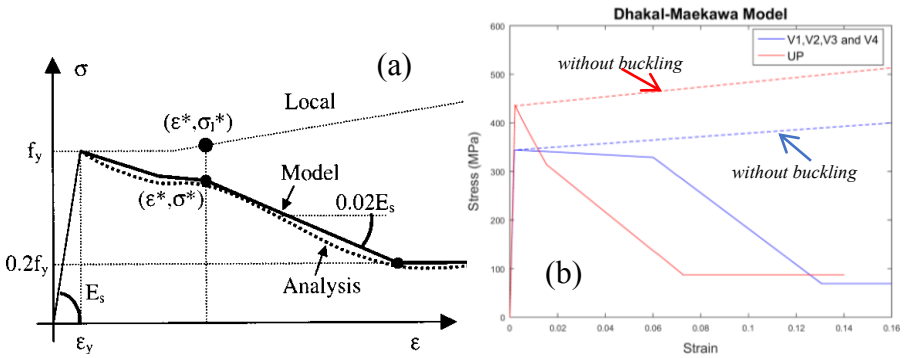

Figure 7: (a) Dhakal-Maekawa proposed buckling model [11] and (b) steel constitutive models for the specimens

Post-yield buckling behavior is included into analyses using Dhakal-Maekawa constitutive models to the bars only under compression. The model is mesh depended and the analyses are carried out after some modifications on the constitutive models according to Dhakal proposal [12]. Figure 8 demonstrates the comparisons of the results in shear and displacement terms. It is clear that the proposed model is sensitive to the mesh sizes and it requires modifications. Nevertheless, the model provides greater agreement with the experimental results in local sense.

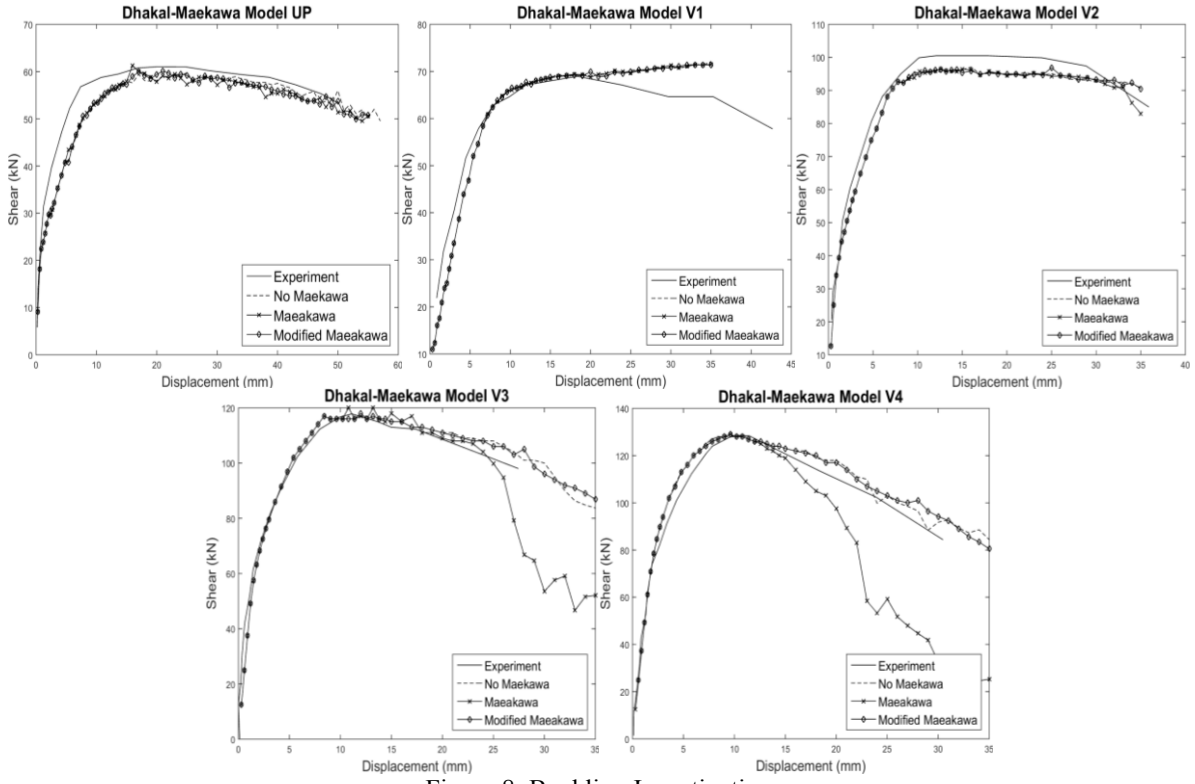

Figure 8: Buckling Investigation

4 CRACK EVOLUTION

In this methodology, bond-slip action is a necessity to match the responses globally and also to form the crack pattern realistically. In Figure 9-Figure 13 the crack patterns are illustrated, including the results from a model without bond-slip, after activating bond-slip and the experimental pictures. All the models are able to reproduce the crack pattern with good agreement. In the model without bond-slip, the crack pattern is more diffuse and there is no clear separation between cracks. On the other hand, the crack pattern from the model with ac-

tive bond-slip is more realistic, the crack widths are greater due to localization. The crack width becomes narrower if the axial load is higher. Finally, Table 2 shows a comparison of damage length from both experiments and finite element analyses, there is satisfactory agreement in the results.

	Damage length (Experimental) *(cm)*	***Damage length (FE)*** *(cm)*
UP	15	15
V1	>20	25
V2	≈21	20
V3	≈20	20
V4	14	15

Table 2: Comparison of the damage length from experiments and FE analyses

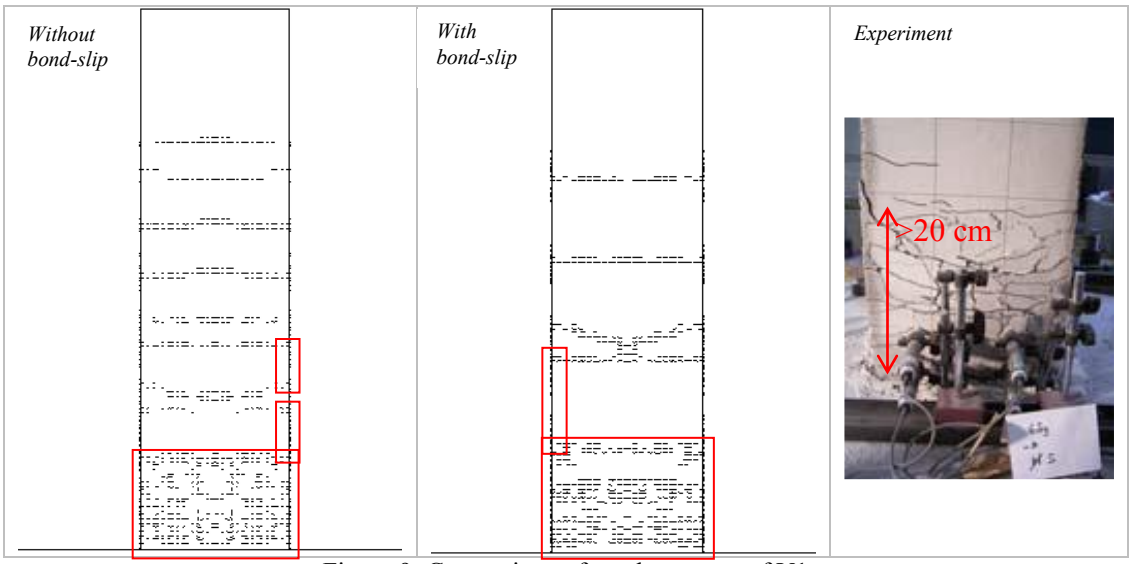

Figure 9: Comparison of crack patterns of V1

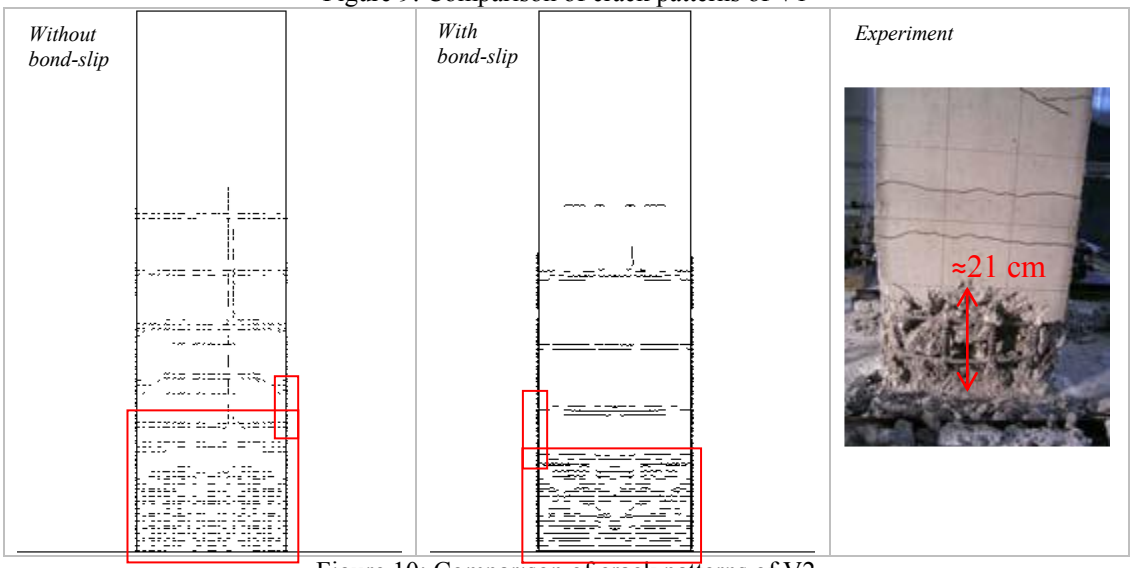

Figure 10: Comparison of crack patterns of V2

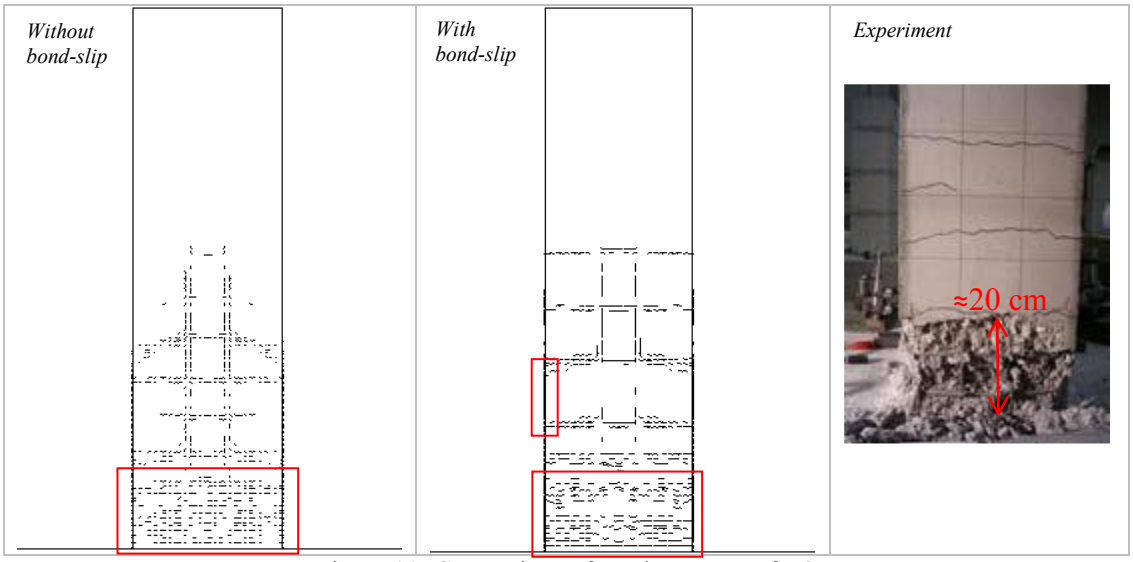

Figure 11: Comparison of crack patterns of V3

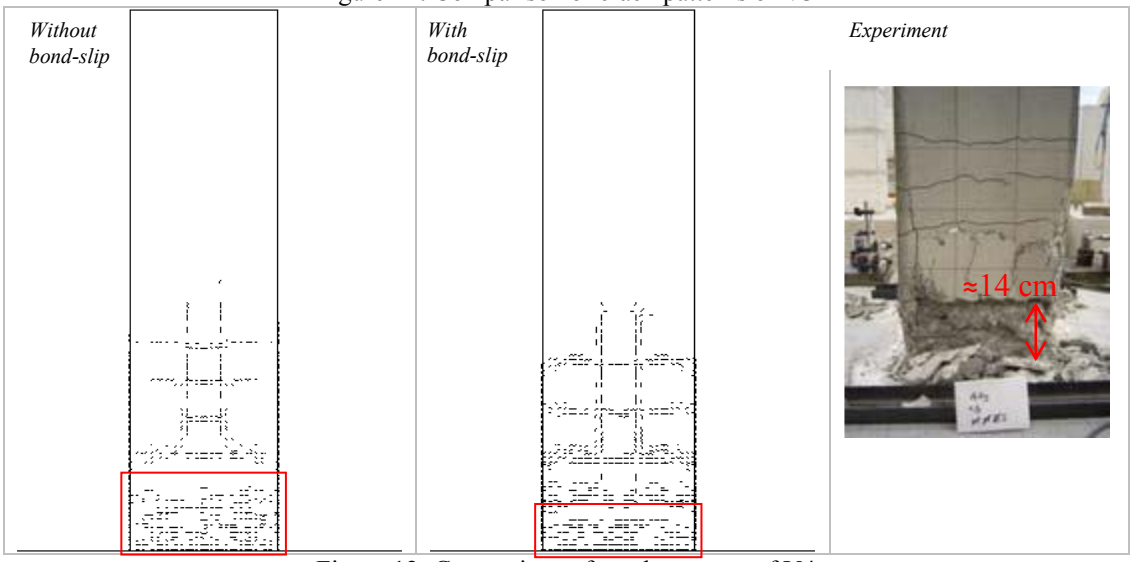

Figure 12: Comparison of crack patterns of V4

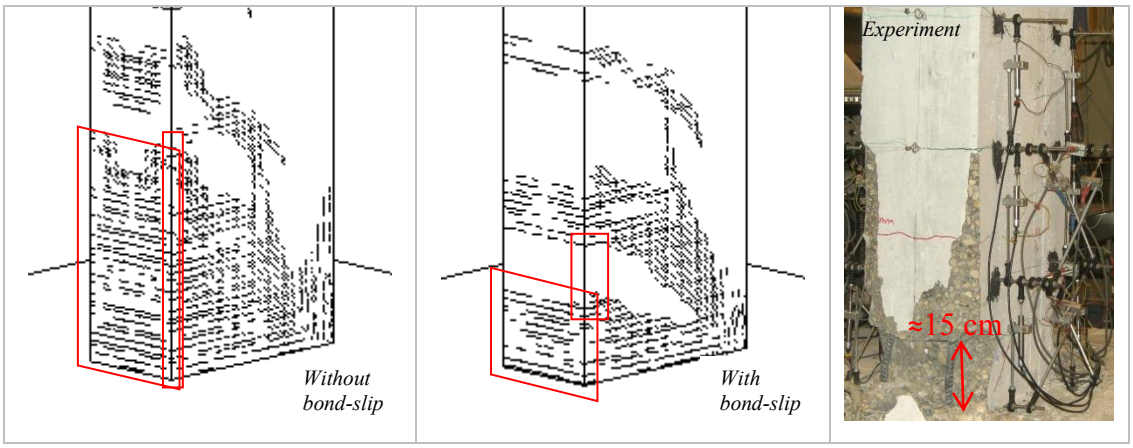

Figure 13: Comparison of crack patterns of UP

5 CONCLUSION

Five columns with different axial load levels, material and geometrical properties are reproduced numerically using DIANA 9.6 and compared with experimental results. To match the numerical and experimental results, a systematic calibration is applied within five steps covering mesh sensitivity analysis, compression fracture energy, geometric nonlinearity, bond-slip activation and rebar buckling. Their effects on the numerical results are discussed in detail and the following conclusions can be obtained:

1- The mesh size has minor influence on peak load and moderate influence on the ductility in case of higher axial load levels;
2- The compression fracture energy plays an important role on ductility in the case of columns subjected to higher axial load levels;
3- Geometric nonlinearity and second order effect shall be considered in the analysis especially if there is a high axial load level;
4- Activation of bond-slip slightly increases the response's ductility and a small reduction in maximum response can be observed. However, it changes significantly the crack pattern;
5- The Dhakal-Maekawa post-yield buckling model provides fair improvement in local response whereas a modification on the constitutive model is applied because of mesh size consideration.

In further steps of the methodology, the physical damages will be correlated with selected engineering demand parameter(s) through numerical models in which the mentioned calibration steps are obeyed.

REFERENCES

[1] A. Cakmak and E. DiPasquale, "Detection and Assessment of Seismic Structural Damage," 1987.
[2] Y. Chung, C. Meyer, and M. Shinozuka, "Seismic damage assessment of reinforced concrete buildings," in *Report No. NCEER-87-0022*, ed: National Center for Earthquake Engineering Research, State University New York at Buffalo, 1987.
[3] Y.-J. Park and A. H.-S. Ang, "Mechanistic seismic damage model for reinforced concrete," *Journal of structural engineering,* vol. 111, pp. 722-739, 1985.
[4] M. S. Williams and R. G. Sexsmith, "Seismic damage indices for concrete structures: a state-of-the-art review," *Earthquake spectra,* vol. 11, pp. 319-349, 1995.
[5] R. Sinha and S. Shiradhonkar, "Seismic Damage Index for Classification of Structural Damage–Closing the Loop," in *Proceedings of the Fifteenth World Conference on Earthquake Engineering*, 2012.
[6] "Earthquake Loss Assessment of the Portuguese Building Stock," University of Porto2014.
[7] T. D. BV. DIANA User's Manual release 9.6 [Online].
[8] H. Rodrigues, "Biaxial Seismic Behavior of Reinforced Concrete Columns," Doctoral Dissertation, Civil Engineering, University of Aveiro, Aveiro, 2012.
[9] T. Denpongpan and H. Shima, "Effect of Axial Load on Ductility of Reinforced Concrete Columns," presented at the OUR WORLD IN CONCRETE & STRUCTURES, Singapore, 2005.

[10] F. I. du Béton, "Bond of reinforcement in concrete: state-of-art report," *Lausanne, Switzerland: International Federation for Structural Concrete,* p. 427, 2000.
[11] R. P. Dhakal and K. Maekawa, "Modeling for postyield buckling of reinforcement," *Journal of Structural Engineering,* vol. 128, pp. 1139-1147, 2002.
[12] R. P. Dhakal, "Enhanced fiber model in highly inelastic range and seismic performance assessment of reinforced concrete," The University of Tokyo, 2000.